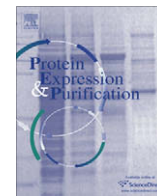




Contents lists available at ScienceDirect

Protein Expression and Purification

journal homepage: www.elsevier.com/locate/yprep

Amalgam, an axon guidance *Drosophila* adhesion protein belonging to the immunoglobulin superfamily: Over-expression, purification and biophysical characterization

Tzviya Zeev-Ben-Mordehai^{a,b}, Aviv Paz^{a,b}, Yoav Peleg^{a,c}, Lilly Toker^b, Sharon G. Wolf^d, Edwin H. Rydberg^e, Joel L. Sussman^{a,c}, Israel Silman^{b,c,*}

^a Department of Structural Biology, Weizmann Institute of Science, Rehovoth 76100, Israel

^b Department of Neurobiology, Weizmann Institute of Science, Rehovoth 76100, Israel

^c Israel Structural Proteomics Center, Weizmann Institute of Science, Rehovoth 76100, Israel

^d Chemical Research Services, Weizmann Institute of Science, Rehovoth 76100, Israel

^e Istituto di Ricerche di Biologia Molecolare P. Angeletti, Pomezia, Italy

ARTICLE INFO

Article history:

Received 4 August 2008

and in revised form 17 September 2008

Available online 8 October 2008

Keywords:

Immunoglobulin
Expression
Secretion
Pichia
Detergent
Multimers

ABSTRACT

Amalgam, a multi-domain member of the immunoglobulin superfamily, possesses homophilic and heterophilic cell adhesion properties. It is required for axon guidance during *Drosophila* development in which it interacts with the extracellular domain of the transmembrane protein, neurotactin, to promote adhesion. Amalgam was heterologously expressed in *Pichia pastoris*, and the secreted protein product, bearing an NH₂-terminal His₆Tag, was purified from the growth medium by metal affinity chromatography. Size exclusion chromatography separated the purified protein into two fractions: a major, multimeric fraction and a minor, dimeric one. Two protocols to reduce the percentage of multimers were tested. In one, protein induction was performed in the presence of the zwitterionic detergent CHAPS, yielding primarily the dimeric form of amalgam. In a second protocol, agitation was gradually reduced during the course of the induction and antifoam was added daily to reduce the air/liquid interfacial foam area. This latter protocol lowered the percentage of multimer 2-fold, compared to constant agitation. Circular dichroism measurements showed that the dimeric fraction had a high β -sheet content, as expected for a protein with an immunoglobulin fold. Dynamic light scattering and sedimentation velocity measurements showed that the multimeric fraction displays a monodisperse distribution, with $R_h = 16$ nm. When co-expressed together with amalgam the ectodomain of neurotactin copurified with it. Furthermore, both purified fractions of amalgam were shown to interact with *Torpedo californica* acetylcholinesterase, a structural homolog of neurotactin.

© 2008 Elsevier Inc. All rights reserved.

Introduction

Multi-domain proteins, which account for over 70% of all eukaryotic proteins, are involved in a wide range of biological processes [1]. While the multiple domains can either be tandem repeats of the same fold or originate from different fold families, bioinformatics analysis suggests that most adjacent domains in multi-domain proteins belong to the latter category [2]. When tandem repeats of the same fold do occur, the two adjacent domains generally have a sequence identity of less than 40%. Interestingly, greater identity has been found to promote co-aggregation [2]. Often, structural characterization of full-length multi-domain proteins is a prerequisite for understanding their function(s);

however, such studies require substantial amounts of pure protein. In most cases, this can only be obtained by over-expression in a heterologous system, which can be challenging for a tandem repeat multi-domain protein, since the effective local protein concentration in the vicinity of each domain is high, making co-aggregation an especial risk [3].

Amalgam (Ama)¹ is a secreted cell adhesion protein in the Antennapedia complex of *Drosophila melanogaster* [4], which is

* Corresponding author. Address: Department of Neurobiology, Weizmann Institute of Science, Rehovoth 76100, Israel. Fax: +972 8 934 6017.

E-mail address: israel.silman@weizmann.ac.il (I. Silman).

¹ Abbreviations used: Ama, Amalgam; IgSF, immunoglobulin superfamily; S2, Schneider 2; Nrt, neurotactin; DmAChE, *Drosophila melanogaster* acetylcholinesterase; TcAChE, *Torpedo californica* acetylcholinesterase; TEV, tobacco etch virus; MD, minimal dextrose; BMMY, buffered methanol complex medium; BMM, buffered minimal methanol; SEC, size-exclusion chromatography; MALDI-TOF, matrix-assisted laser desorption/ionization time-of-flight; Endo F1, endoglycosidase F1; GST, glutathione S-transferase; FPLC, fast performance liquid chromatography; MW, molecular weight; CD, Circular dichroism; DLS, Dynamic light scattering; EM, Electron microscopy.

responsible for specifying correct embryonic head and thoracic segmental identity. Immunostaining studies localized it to the extracellular surface of various mesodermal and neuronal cells during embryogenesis [4]. Ama is a member of the immunoglobulin superfamily (IgSF), a large group of proteins involved in many biological processes, including the immune response and various aspects of cell surface recognition [5]. As implied by the name, all proteins in this superfamily contain a conserved Ig domain, which contains ~100 amino acids, and forms a sandwich of two β -sheets that are typically stabilized by a single conserved intrachain disulfide [6]. IgSF members often contain more than one domain; indeed, Ama consists of three Ig domains. These domains are 18–32% identical to each other in pairwise comparisons, and the sequences displaying the greatest identity are centered around the pairs of conserved cysteines that form the intrachain disulfide bonds. Sequence analysis predicts three N-linked glycosylation sites, two in the first and one in the third domain.

The *ama* gene encodes a 333-amino-acid polypeptide, which is predicted to have an NH₂-terminal signal sequence, three Ig domains, and a short COOH-terminal segment. Schneider 2 (S2) cells transfected with the *ama* gene secrete Ama into the medium [7]. Use of this medium in a cell aggregation assay showed that Ama possesses heterophilic adhesion properties, and serves as a ligand for the neuronal adhesion protein, neurotactin (Nrt) [7], a type-II transmembrane glycoprotein which functions as a heterophilic cell adhesion molecule in axon pathfinding and fasciculation [8,9]. Nrt has a 500-amino-acid extracellular domain with 30% and 31% identity, respectively, to *Drosophila melanogaster* acetylcholinesterase (*DmAChE*) and *Torpedo californica* acetylcholinesterase (*TcAChE*) [8], and a 324-amino-acid cytoplasmic domain which has been assigned to the class of intrinsically disordered proteins [10]. Ama is required both for primary cultures of embryonic cells to associate and for Nrt-expressing S2 cells to aggregate [7]. Further aggregation assays performed with Ama engineered to be expressed on the plasma membrane of S2 cells showed that Ama also possesses homophilic adhesion properties [11]. Using an Ama-deficient stock it was shown that Ama function is not essential for viability, but that pupae deficient in Ama exhibit defasciculation defects, i.e. defects in the dissociation of axon bundles of the ocellar nerves similar to those found in Nrt mutants [11].

Here we report the over-expression of Ama, a multi-domain protein with three immunoglobulin (Ig) domain repeats, in the methylotrophic yeast, *Pichia pastoris*. Its purification, and biochemical and biophysical characterization are also presented.

Materials and methods

Materials

The *Pichia* expression vector and strain were from Invitrogen (Carlsbad, CA). Yeast extract and peptone were from Pronadisa Conda Laboratories (Madrid, Spain). Yeast nitrogen base was from Difco (Lawrence, KS). Anti-His-tag antibodies, antifoam C, biotin, BSA, sorbitol, KH₂PO₄, K₂HPO₄, NaH₂PO₄, Na₂HPO₄, imidazole and decamethonium bromide were from Sigma (St. Louis, MO). Gentamicin (G418) was from Gibco (Grand Island, NY). Zwittergent 3–12 and CHAPS (3-[(3-cholamidopropyl)dimethylammonio]-1-propanesulfonate) were from Calbiochem (Darmstadt, Germany). The analytical Superdex200 HR 10/30 column, HiLoad 26/60, Superdex200pg, CNBr-activated Sepharose 4B and the Ni Sepharose 6 Fast Flow column were all from General Electric Healthcare (Uppsala, Sweden). GelCode Blue Stain and GelCode glycoprotein staining kit were from Pierce (Rockford, IL). *TcAChE* was the dimeric (G₂) glycosylphosphatidylinositol-anchored form purified from electric organ tissue of *Torpedo californica* by affinity chromatography on a *m*PTA-Sepharose column subsequent to solubiliza-

tion with phosphatidylinositol-specific phospholipase C [12]. Anti-Ama antibodies were raised by the Weizmann Institute Biological Services Antibody Unit.

Cloning

The gene fragment encoding full-length *D. melanogaster* Ama (GenBank accession no. CG2198, residues 24–333, without the putative signal peptide) and the gene fragment encoding the ecto-domain of *D. melanogaster* Nrt (Nrt-ext; GenBank accession no. CG9704, residues 347–846) were amplified using standard PCR methods from *ama* cDNA and *nrt* cDNA, respectively, both of which were a gift from Dr. Michel Piovant (Université de la Méditerranée, Marseille, France). The primers used for amplification introduced EcoRI and NotI restriction sites at the 5' and 3' ends, respectively, and, in the case of Ama, also introduced a 5'-His₆-tag coding sequence, followed by a recognition site for cleavage by the tobacco etch virus (TEV) protease [13] (Table 1). The PCR amplification products of *ama* and *nrt* were cloned in-frame into the corresponding EcoRI and NotI sites on the *Pichia* expression vectors pPIC9K and pPICZ α , respectively, containing the α factor secretion signal [14]. The resulting expression vectors were designated pPIC9K/*ama* and pPICZ α /*nrt-ext*. Integrity of the coding sequences was confirmed by the Weizmann Institute Biological Services DNA Sequencing Facility.

Establishment of stable *Pichia* recombinant clones for the expression of Ama

pPIC9K/*ama* was linearized with SacI, and transformed by electroporation according to the Invitrogen protocol. Briefly, electrocompetent *P. pastoris* GS115 cells were freshly prepared before transformation by consecutive washing with ice-cold sterile water and 1 M sorbitol. For transformation, 120 μ L of electro-competent GS115 cells were incubated for 5 min with 1 μ g of the linearized vector in a 0.2 cm electroporation cuvette. A single 1.5 kV pulse was employed, with a capacitance of 25 μ F, a resistance of 200 Ω , and a time constant of 4.5 ms. Following the pulse, 1 mL of 1 M ice-cold sorbitol was added, and the cells were plated on minimal dextrose (MD) plates. Single colonies isolated from the MD plates were directly screened for the *ama* gene by colony PCR, using 5' and 3' AOX1 primers (Invitrogen, Carlsbad, CA) (Haaning 1997).

Screening for multiple integration events and for the highest expression clone

Multiple plasmid integration events occur spontaneously in *Pichia* at a low but detectable frequency. The *in vivo* method of screening for such events utilizes hyper-resistance to the antibiotic G418 [14]. The vector used, pPIC9K, contains the bacterial kanamycin gene that confers resistance to G418 in *Pichia*. The level of G418 resistance roughly correlates with the number of kanamycin cassettes integrated. GS115/pPIC9K/*ama* clones were thus collected and re-plated on YPD plates containing increasing concentrations of G418, namely 0.25, 0.5, 1.0, 2.0, 3.0 and 4.0 mg/mL. All clones

Table 1
List of primers.

Ama	Upper	5'-CGTAGAATTCATCATCATCATCATCATAGCAGCGAAAACCTGTACTTCCAGGGT GCCCCAGTGATCAGCCAGATC
	Lower	5'-CTAATTCGCGGCCGCTTACGACAAGGAGGGCACTGGGAT
Nrt-ext	Upper	5'-CGTAGAATTCACGAGACTTTGACCTCGCCG
	Lower	5'-CTAATTCGCGGCCGCTTAAATCGACGGCGCATACCCGG

that grew on 4 mg/mL G418 plates were checked for expression following the Invitrogen protocol for small-scale expression; expression was detected by Western blotting using anti-His-tag antibodies.

Establishment of stable Pichia recombinant clones for co-expression of Ama and of the extracellular domain of Nrt

The expression vector *pPICZα/nrt-ext* was transformed by electroporation into the GS115/*pPIC9K/Ama* clone used for Ama expression, with selection being performed on YPD plates containing 2 mg/mL Zeocin. Several clones were checked for expression following the Invitrogen protocol for small-scale expression.

Small-scale expression

The *ama* clone displaying the highest expression levels using the above screening procedure was cultured in 50 mL of buffered glycerol complex medium (BMGY) at 30 °C in a 250 mL baffled flask. After 24 h, the cells were harvested by centrifuging at 1500g for 5 min at room temperature. The supernatant was decanted, and expression was induced by resuspending the cell pellet in a 250 mL baffled flask to $OD_{600} = 1.0$ in 50 mL of one of the following media: buffered methanol complex medium (BMMY), buffered minimal methanol (BMM) or minimal methanol (MM) (see Invitrogen manual for composition). Resuspension was followed by incubation for up to 6 days at either 20 or 30 °C, with daily addition of 1% methanol. For the buffered media, four pH values were tried, *viz.*, 5.0, 6.0, 7.5 and 8.5. For expression in the presence of detergent, either Zwittergen 3–12 (0.05 or 0.1% v/v) or CHAPS (2, 4, 6, or 8 mM) was added one day after protein induction. An aliquot (1 mL) was taken from the growth medium daily, and the expression level was analyzed by Western blotting using anti-His-tag antibodies. For evaluation of the effects of added detergent, the multimer/dimer ratio was analyzed by size-exclusion chromatography (SEC) on an analytical Superdex200 HR 10/30 column.

Large-scale expression of Ama

A pre-culture in 10 mL YPD was started from a fresh YPD plate containing the GS115/*pPIC9K/ama* clone, and cultivated for 18 h at 30 °C. The starter was diluted into 0.5 L BMGY in a 2 L baffled flask, followed by incubation at 30 °C for 24 h. Cells from an aliquot of 50 mL from the BMGY culture were harvested by centrifugation at 1500g for 5 min at room temperature. The supernatant was decanted, and expression was induced by resuspending the cell pellet in 0.5 L of either BMM or BMMY, both at pH 5.0 in a 2 L baffled flask. Induction was maintained for 5 days at 20 °C by daily addition of 1% methanol. Antifoam was either added as a single aliquot of 0.2 mL at the commencement of induction, or as 4 daily 0.05 mL aliquots, starting 24 h after commencement of induction. Agitation was either maintained at 170 rpm, or initiated at 220 rpm, and lowered by 20 rpm each day. After 120 h, the growth medium was separated from the cells by centrifugation at 6500 rpm for 15 min.

Purification of Ama

The growth medium was titrated to pH 8.0 with 10 M KOH, and centrifuged at 6500 rpm for 15 min, after which a 1 L volume of the culture was loaded onto a 15 mL Ni Sepharose 6 Fast Flow column. The column was washed with 10 column volumes of buffer A (0.5 M NaCl/20 mM NaHPO₄, pH 8.0), supplemented with 20 mM imidazole, and the protein was then eluted with 3 column volumes of buffer A supplemented with 0.5 M imidazole. The eluant was filtered through a 0.22 μm PES membrane (Whatman, Kent, UK), con-

centrated 10-fold using a 15 mL 30 kDa MWCO filter (Amicon Billerica, MA), and loaded onto a HiLoad 26/60 Superdex200pg SEC column that had been pre-equilibrated with buffer A. The protein concentration was estimated from the absorbance at 280 nm in a nanodrop spectrometer (NanoDrop Technologies, Wilmington, DE), using a molar extinction coefficient of 30,230 M⁻¹ cm⁻¹ (estimated using ExPASy proteomics tools, <http://www.expasy.ch/tools>). Determination of mass and peptide mapping analysis, using matrix-assisted laser desorption/ionization time-of-flight (MALDI-TOF), were performed by the Weizmann Institute Biological Services Mass Spectrometry Laboratory.

Deglycosylation of Ama

The glycans were removed from Ama dimers enzymatically, using recombinant endoglycosidase F1 (Endo F1) tagged with glutathione *S*-transferase (GST) [15]. Ama was incubated with 1% (w/w) of Endo F1 for 48 h at 25 °C in buffer A titrated to pH 5.6 with 0.5 M sodium acetate, pH 4.5. To remove Endo F1, following sample clarification by centrifugation at 14,000 rpm for 20 min, and pH correction to pH 9.0 with 1 M Tris-HCl, the sample was passed through a 1 mL HiTrap Glutathione HP column.

Isoelectric focusing (IEF)

IEF was performed on a precast IEF gel with a pH range of 5–8 (Bio-Rad, Hercules, CA) employing the PROTEAN II system (Bio-Rad, Hercules, CA). Before application, samples (1 mg/mL) were diluted 2-fold with 50% glycerol. The gels were stained with IEF Gel Staining Solution (Bio-Rad, Hercules, CA).

Molecular weight determination by SEC

Gel filtration was performed on an analytical size-exclusion column (Superdex200) equilibrated with buffer A, using an AKTA fast performance liquid chromatography (FPLC) system (General Electric, Uppsala, Sweden). The elution volume (V_e) was monitored by absorbance at 280 nm. V_e for a particular molecular species was then converted to K_{av} by use of the following equation:

$$K_{av} = \frac{V_e - V_0}{V_t - V_0}$$

where V_0 is the exclusion volume, taken as the elution volume of dextran blue, and V_t is the total bed volume. The molecular weight (MW) of the Ama dimer was calculated using a linear calibration plot of log MW vs. K_{av} obtained with a standard globular protein kit.

Interaction of Ama with TcAChE

For this study, the *m*PTA-Sepharose resin used for affinity purification of TcAChE was employed [12]. After absorption of TcAChE, the column was washed with buffer B (20 mM NaHPO₄, pH 7.2). Aliquots from this resin (600 μL, 50% suspension) were incubated overnight at 4 °C with 300 μL (0.1–0.5 mg/mL) of either dimeric, multimeric, or deglycosylated Ama. BSA (0.5 mg/mL in buffer B) similarly incubated with the resin, served as a control. A further control involved incubation of the two Ama fractions under the same conditions with 600 μL of *m*PTA-Sepharose that had not been exposed to TcAChE. Following incubation, the resins were transferred to Bio-spin columns and centrifuged at 2000 rpm at 4 °C for 30 s to wash out the unbound proteins. AChE activity was checked in the flow-through fractions to confirm that the enzyme had not leaked from the column. The columns were then washed with 30 CV of buffer B, followed by elution of TcAChE with 100 μL of 10 mM decamethonium in buffer B (*viz.*, the same concentration of decamethonium as used for its elution in the purifica-

tion procedure [12]). All fractions were blotted with anti-Ama antibodies at a 1:10,000 dilution.

Circular dichroism (CD) spectroscopy

CD spectra were recorded on an AVIV Model 202 CD spectrometer (AVIV Biomedical, Lakewood, NJ). Far-UV spectra were recorded in a 0.1-cm path length cell. All CD spectra were recorded in 10 mM Na₂HPO₄, pH 8.0, at a protein concentration of 15 μ M, at 25 °C, with a step size of 0.25 nm and an averaging time of 3 s. Each spectrum shown is derived from three spectra that were accumulated, averaged, and corrected for the contributions of the buffer.

Dynamic light scattering (DLS)

DLS measurements were performed on a Viscotek 802 instrument (Houston, TX) in buffer A, at a protein concentration of 1 mg/mL.

Analytical ultracentrifugation

Sedimentation velocity experiments were carried out on a Beckman Optima XL-A analytical ultracentrifuge (GMI, Ramsey, MN) in an An-50Ti rotor. Aliquots (400 μ L) of Ama multimers in buffer A, and of buffer A, were injected into a double-sector cell with a 12 mm Epon centerpiece and quartz windows. Ultracentrifugation was performed at 50,000 rpm and 21 °C (following a 6-h temperature equilibration period). The absorbance wavelength was 230 nm, at which wavelength the Ama solution had an absorbance of 0.5. A radial step size of 0.003 was used for scanning, and 200 scans were collected, at which point sedimentation was complete. Data from all scans were analyzed using the SEDFIT program [16], with a continuous sedimentation coefficient $c(s)$ distribution model. The solvent density, the partial specific volume and the R_H were obtained using the SEDNTERP program [17].

Electron microscopy (EM)

Ama was deposited on carbon-coated glow-discharged electron microscope grids at a concentration of 50 μ g/mL. The grids were then stained with 2% uranyl acetate. Microscopy was performed at 120 kV with an FEI Tecnai T12 electron microscope (FEI, Hillsboro, OR), and images were recorded using an FEI Eagle camera.

Results

Construction of stable *Pichia* transformants containing multiple copies of the Ama gene

Despite extensive screening of expression conditions, full-length Ama expressed only as inclusion bodies in *Escherichia coli* (data not shown). Since this was probably due to the absence of post-translational modifications, the yeast *P. pastoris* was selected as a eukaryotic expression system. The gene encoding for full-length Ama, but without the putative signal peptide, was cloned into pPIC9K, and subsequently transformed and integrated into the genome of the *Pichia* strain GS115 (*his*⁻). *His*⁺ transformants were selected by their ability to grow on minimal medium lacking histidine. Several such clones that were tested for small-scale expression did not display detectable expression of Ama (data not shown). Multiple-copy integration of recombinant genes in *Pichia* has, in some cases, been shown to increase expression of the desired protein due to a gene dosage effect [14]. The vector used permits detection of multiple integration events by screening for clones that are hyper-resistant to the antibiotic, G418. Ama

expression was detected by SDS-PAGE for clones that grew on a plate containing 4 mg/mL of G418, which corresponds to 7–12 copies of the expression cassette (Fig. 1I). One of these clones was selected for use in all subsequent expression experiments.

Since *Pichia* does not secrete many endogenous proteins, Ama is clearly detected on SDS-PAGE even before purification, exhibiting an apparent MW of ~45 kDa (Fig. 1I). The MW was found to be $[M+H]^+ = 44,619$ Da by MALDI mass spectrometry (MS); peptide mapping, also using MALDI-MS, matched 44% of the tryptic fragments to Ama (data not shown). However, the theoretical MW based on the amino-acid sequence, is 36,675 Da (including the His₆-tag and TEV recognition site). This discrepancy was ascribed to glycosylation; indeed, Fig. 1II shows that the Ama band could be stained using the GelCode glycoprotein staining procedure. Furthermore, N-terminal sequencing confirmed that the signal peptide was removed (not shown).

Screening for optimal expression conditions

Secretion of Ama into the growth medium is directed by the *Saccharomyces cerevisiae* α factor prepro peptide, which is removed by the KEX2 protease [18]. Culture conditions, including temperature, medium composition, various additives and, in particular, pH, have a substantial impact on levels of secreted protein in *Pichia* [18]. Since the secreted protein accumulates in the growth medium during protein production, its biophysical properties, in particular its *pI* and stability, should be taken into consideration in selecting the medium and its pH. Accordingly, a matrix of conditions, including growth temperature, medium type and pH, was screened for optimal expression conditions. By 72 h following initiation of induction with methanol, Ama can be detected in most media and pH values tested, using SDS-PAGE and Western blotting (representative Western blots are shown in Fig. 2). High expression levels are obtained in either BMM, pH 5.0, at 30 °C, or in BMM and BMMY, pH 5.0, at 20 °C. However, Western blots reveal the pres-

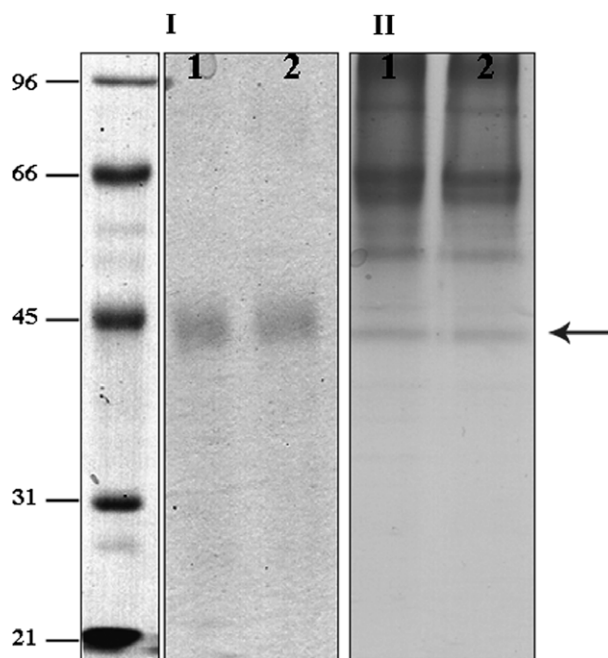


Fig. 1. Detection of secreted Ama in the *Pichia* culture medium. Fifteen microliters samples of each culture medium were subjected to SDS-PAGE, and analyzed using: (I) GelCode protein staining; (II) GelCode glycoprotein staining kit; 1, 120 h induction in BMM, pH 5.0; 2, 144 h induction in BMM, pH 5.0. The arrow on the right indicates the position of Ama.

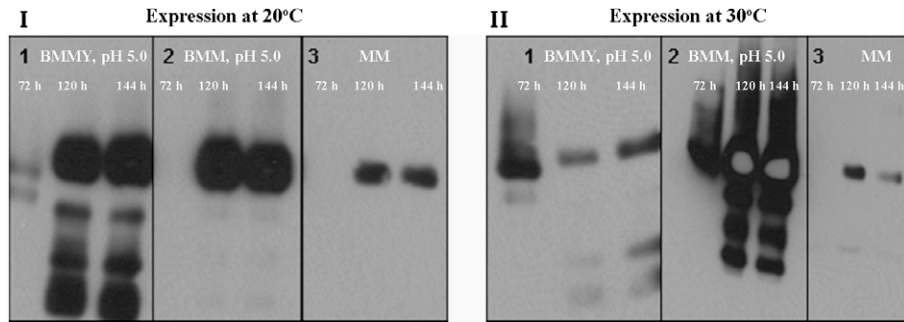


Fig. 2. Screening of conditions for Ama expression. (I) expression at 20 °C; (II) expression at 30 °C. 1, BMMY, pH 5.0; 2, BMM, pH 5.0; 3, MM. For each set of conditions the left lane corresponds to 72 h induction, the middle lane to 120 h induction, and the right lane to 144 h induction. Visualization utilized Western blotting with an anti-HisTag antibody.

ence of lower MW bands which are most likely degradation products of the full-length Ama for the expression in BMM, pH 5.0, at 30 °C and BMMY, pH 5.0, at 20 °C (Fig. 2). Both BMMY and BMM at pH 5.0 and 20 °C were further compared under large-scale expression conditions (see below).

Ama is expressed as dimers and multimers

Purification to near homogeneity was achieved in two steps, metal affinity chromatography, making use of the His₆-tag, followed by SEC. Ama is >95% pure after the first step of purification, but displays heavy smearing upon SDS-PAGE under reducing conditions (Fig. 3A, lane 2). The pooled fractions of the eluant from the affinity column were further separated by SEC into two fractions. The major one, eluting in the void volume of the column, was multimeric, and the minor one eluted at a position corresponding to the molecular weight of a dimer, ~90 kDa (Fig. 3B). These two fractions were produced whether expression was in BMM or in BMMY, but with different dimer/multimer ratios (see Table 2). Multimer formation precedes purification, since an aliquot loaded directly from the medium onto an SEC column also separates into two fractions (Fig. 3B). There is no observed equilibrium between the two fractions. Thus, the dimeric fraction can be concentrated to high concentrations with no formation of multimers, and no dimers are detected upon repeated SEC of the multimer fraction.

Expression in the presence of detergent greatly decreases the multimer fraction

Native PAGE was used to screen for the effects of various detergents on the degree of multimerization of Ama. The purified multimers were incubated with each detergent for 30 min prior to native PAGE. The two zwitterionic detergents, Zwittergent 3–12 and CHAPS, were the only ones tested able to achieve partial conversion to monomers (data not shown). It was previously shown that Tween-20 could be used to inhibit protein aggregation during *Pichia* fermentation [19], and with the notion that it might be easier to prevent formation of the multimers than to dissociate them we added these detergents directly to the *Pichia* culture medium. Both detergents were added at several concentrations to the BMM, pH 5.0 medium. While culture growth was inhibited even by concentrations of Zwittergent 3–12 as low as 0.05%, growth was not affected even at CHAPS concentrations as high as 8 mM. The detergent was added only 24 h after induction had been initiated, so as to allow the culture to reach a high density prior to Ama expression. Fig. 4A shows that Ama expressed in the presence of 6 mM CHAPS is produced mainly as the dimer. Table 2 summarizes the multimer/dimer ratios for the various detergent concentrations. In cases in which large-scale production and purification had been carried out, the total amounts of purified dimer obtained are listed.

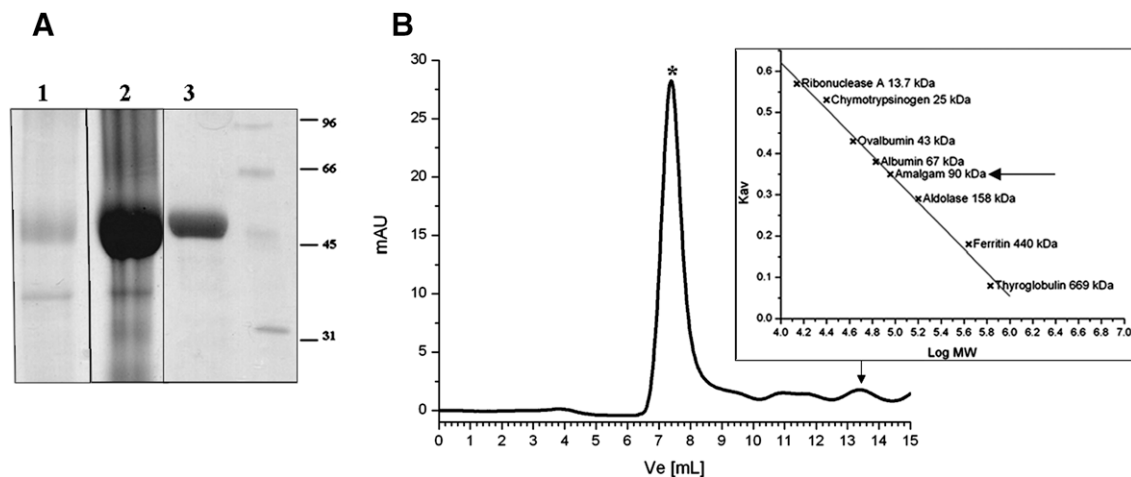


Fig. 3. Ama purification from large-scale expression in BMMY, pH 5.0. (A) 1, Concentrated medium; 2, Pooled fractions eluted from the metal affinity column; 3, Dimeric fraction after SEC on Superdex200. (B) Analytical SEC on Superdex200 of an aliquot taken directly from the expression medium (BMM, pH 5.0). The elution pattern reveals a major multimeric peak eluting in the void volume at 7.7 mL, indicated by an asterisk, and a minor dimeric form eluting at 13.5 mL, indicated by an arrow. (Insert) Calibration plot for analytical Superdex200 of log MW vs. K_{av} obtained with globular protein markers. The position of dimeric Ama on this plot is indicated by an arrow.

Table 2

Dimer/multimer ratios and total yields of Ama dimer for the various expression conditions tested at 20 °C.

	Medium	Antifoam [mL]	Shaking ^a	Detergent	Dimer/multimer ratio ^b	Total yield of Ama dimer ^c [mg]
1	BMM pH 5.0	0.2	C	—	1/10	2.5
2	BMM pH 5.0	0.2	C	0.05%/0.1% Zwittergent 3–12	ND ^d	—
3	BMM pH 5.0	0.2	C	2 mM CHAPS	1/5	— ^e
4	BMM pH 5.0	0.2	C	4 mM CHAPS	1/2.5	— ^e
5	BMM pH 5.0	0.2	C	6 mM CHAPS	1/0.2	2
6	BMM pH 5.0	0.2	C	8 mM CHAPS	1/0.5	— ^e
7	BMMY pH 5.0	0.2	C	—	1/5	3.5
8	BMMY pH 5.0	0.05 × 4 ^f	NC	—	1/2	6.5

^a Shaking was either constant (C), at 170 rpm, or not constant (NC) i.e. initiated at 220 rpm, and decreased daily by 20 rpm.

^b An aliquot from the medium was loaded directly on to a SEC column, and the dimer/multimer ratio was determined on the basis of the areas under the peaks. The values shown represent average values for several productions.

^c The amounts of protein shown in the last column are those obtained from 1 L culture after the two purification stages, viz., nickel-column chromatography followed by SEC, and represent average values for several productions.

^d Culture growth was inhibited by the detergent, and no Ama could be detected.

^e Tested only on a small-scale. Consequently, the Ama was not purified, and total amounts of dimer could not be determined.

^f Antifoam was added daily, as small aliquots (0.05 mL), starting 24 h after induction.

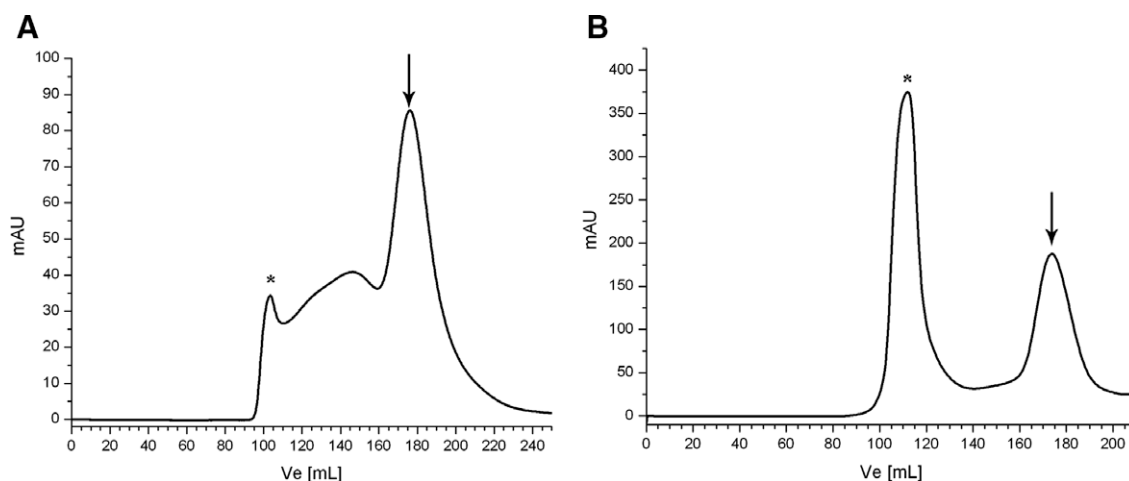


Fig. 4. Preparative SEC of Ama. (A) After expression in BMM, pH 5.0, in the presence of 6 mM CHAPS; (B) after expression in BMMY, pH 5.0, with gradual lowering of the agitation rate together with daily addition of antifoam. Arrows and asterisks indicate the dimeric and multimeric fractions, respectively.

Gradual lowering of the agitation rate together with daily addition of antifoam decreases the multimeric fraction

Minimizing shearing force and reducing the air/liquid interfacial foam area have been shown to be important factors for reducing protein aggregation during secretory expression in yeast bioreactor cultures [20]. We tried to apply a similar approach to our shaking flask procedure. During initial attempts at large-scale expression in BMMY, pH 5.0, we observed that if a slow shaking rate was applied from the beginning of induction the culture did not reach a high density. Likewise, if the entire amount of antifoam needed to reduce foaming throughout the course of the induction was added at the beginning of induction, in this case, too, the culture did not reach high density. Therefore, a protocol was adopted in which agitation was gradually decreased during the course of induction, and small amounts of antifoam were added daily. Under these conditions, the dimer/multimer ratio was increased 2.5-fold, and the amount of purified dimer obtained increased almost 2-fold (Table 2, Fig. 4B).

Glycosylation of dimeric Ama

As was shown by the glycoprotein staining, Ama secreted from *Pichia* is glycosylated (Fig. 1). *Pichia* mainly forms *N*-glycans with a Man₈₋₁₁GlcNAc₂ core structure [21]; this core structure corre-

sponds to a molecular weight of ~1.7–2.2 kDa. As noted in the Introduction, Ama has three *N*-glycosylation sites, NCT, NVT, and NAT, at Asn45, Asn86 and Asn308, respectively. When purified dimeric Ama was treated with Endo F1, its MW was reduced from 44,619 to 38,533 Da as determined by MS (Fig. 5). Fig. 5A shows that a similar reduction in apparent MW, from ~45 to ~38 kDa, is also seen on SDS-PAGE. This reduction of ~6 kDa in apparent MW produced by treatment with Endo F1 correlates with Ama having three *N*-glycosylation sites and with the size of the *N*-linked oligosaccharide associated with such sites. Even after removal of the *N*-linked glycans, the mass of the recombinant Ama is ~2 kDa greater than the MW calculated from the amino acid sequence. This extra mass may, perhaps, be accounted for by *O*-linked glycosylation, which is known to occur in *Pichia* [21,22].

The Ama dimer is fairly homogenous in terms of MW, as can be seen on SDS-PAGE (Fig. 3A). However, it is heterogeneous in terms of its *pI*, as revealed by IEF (Fig. 5D). Before deglycosylation with Endo F1, six distinct isoforms are seen. After removal of the *N*-glycans the number of isoforms was reduced to three, indicating that the heterogeneity is in part due to glycosylation. The *N*-linked core attached by *Pichia* is not charged; however, additional processing of the core glycans by attachment of phosphate to mannose residues, occurs in most yeasts, and phosphorylated oligosaccharides, both *N*- and *O*-linked, have been detected on glycoproteins expressed in *Pichia* [22]. Thus, the *pI* heterogeneity observed for

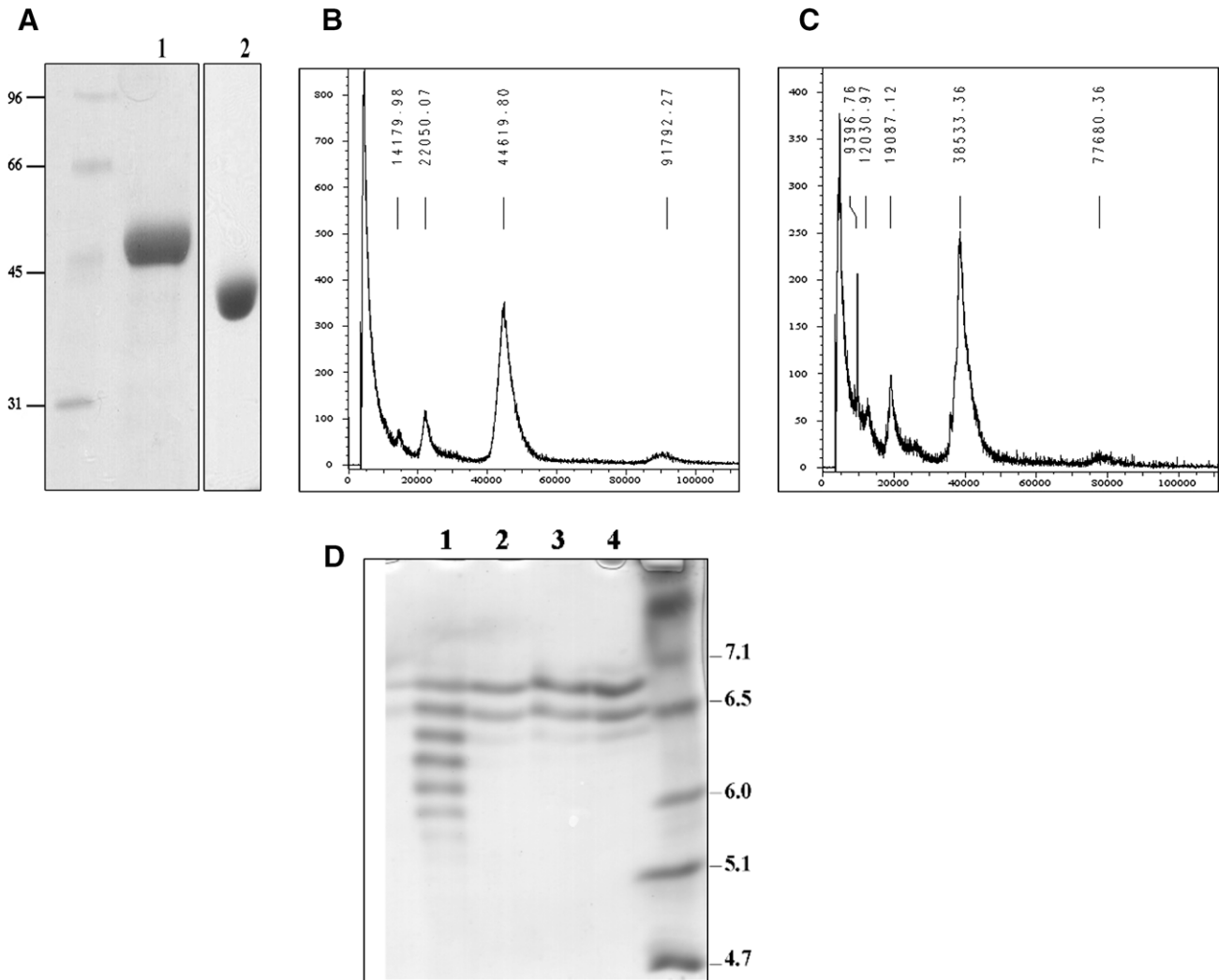


Fig. 5. Deglycosylation of dimeric Ama with Endo F1. (A) SDS-PAGE: Lane 1, before deglycosylation; lane 2, after deglycosylation. (B) MS profile of dimeric Ama before deglycosylation. (C) MS profile of dimeric Ama after deglycosylation. (D) Isoelectric focusing: Lane 1, before deglycosylation; lanes 2–4, after deglycosylation.

Ama may be ascribed in part to phosphorylation of the oligosaccharides. The source of the residual heterogeneity remains to be determined.

Interaction of Ama with Nrt-ext and TcAChE

The functional status of Ama was first examined by testing its capacity to copurify with Nrt-ext when co-expressed with it. The Nrt-ext gene, without a metal affinity tag, was transformed into the GS115/pPIC9K/Ama *Pichia* strain which expressed Ama with a metal affinity tag at its N-terminus. Fig. 6, lane 1, shows that the two proteins were co-expressed two days after initiation of induction with methanol. One dominant broad band was observed on SDS-PAGE of a fraction eluted from the metal affinity column with 0.5 M imidazole (Fig. 6, lane 2). MALDI-MS revealed that this band contained both Ama and Nrt peptides as identified by peptide mapping analysis, with 33% and 29% coverage, respectively. Since only the Ama bore a His₆-tag, whereas Nrt-ext did not, these data show that the two proteins were not only co-secreted but also formed a complex.

Darboux and coworkers reported that S2 cells expressing chimeras in which the AChE-like ectodomain of Nrt had been replaced by the homologous domain of either *Dm*AChE or *Tc*AChE aggregated similarly to cells expressing wild-type Nrt [23]. This

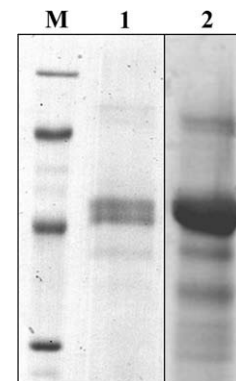


Fig. 6. Co-expression of NRT-ext and AMA. Lane 1, aliquot from the growth medium; lane 2, fraction eluted from the metal affinity column.

provided strong evidence that both these AChEs could recognize Ama similarly to the ectodomain of Nrt. Accordingly, we examined the ability of the purified dimeric and multimeric fractions of Ama to interact with *Tc*AChE. Samples of both were passed through a *m*PTA-Sepharose affinity column routinely used for purification of *Tc*AChE [12] to which the enzyme had previously been bound

(see Materials and methods). The columns were washed with low-ionic-strength buffer, followed by 10 mM decamethonium in the same buffer, which would be expected to elute the bound TcAChE as in the normal purification procedure [12]. Eluant fractions were Western blotted with anti-Ama antibodies, revealing that both the dimeric and multimeric species of Ama coeluted with TcAChE from the affinity column. The results obtained are shown in Fig. 7. It was also shown that Ama deglycosylated with Endo F1 interacted specifically with TcAChE (Fig. 7). This experiment shows qualitatively that both the dimeric and multimeric fractions of Ama are functional in the sense that both can interact specifically with the TcAChE, and that this interaction does not appear to involve the N-glycans. A control experiment showed that Ama did not bind significantly either to an mPTA column that had not been preincubated with TcAChE or to glutathione–Sephacel to which Endo F1-GST had been bound.

Physicochemical characterization

The Ama multimers that form in the course of expression in *Pichia* are both soluble and stable, and do not precipitate even at a concentration of 18 mg/mL, which permits their biophysical characterization alongside the dimer.

The far-UV CD spectra of the two fractions of Ama are presented in Fig. 8. That of the dimer has an ellipticity minimum at 218 nm, and zero ellipticity at 206.5 nm, indicating a high β -sheet content, as expected for an Ig-domain protein [24]. However, in the CD spectrum of the multimeric fraction, the characteristic minimum at 218 nm both broadens and shifts to a lower wavelength (212 nm), and the spectrum displays a negative ellipticity at 206.5 nm, suggesting an increased random coil content relative to the dimer.

Sedimentation velocity measurements in an analytical ultracentrifuge (AUC-SV) for the multimer fraction gave a sedimentation coefficient peak at 14S (Fig. 9A), corresponding to a hydrodynamic radius, R_H , of 18 nm. However, the broadness of the distribution indicates a certain degree of heterogeneity. DLS measurements also showed that the multimer fraction displays a monodisperse distribution (Fig. 9B), with an R_H value of 16 nm.

The multimer particles were further negatively stained with uranyl acetate and visualized by EM. The negatively stained multimers appeared mostly as non-perfect circular particles with a heterogeneous distribution of diameters ranging from 10 to 20 nm, and thus were unsuitable for 3D reconstructions (Fig. 10). The size of the particles seen in the EM is about 2-fold smaller than the values obtained using the biophysical tech-

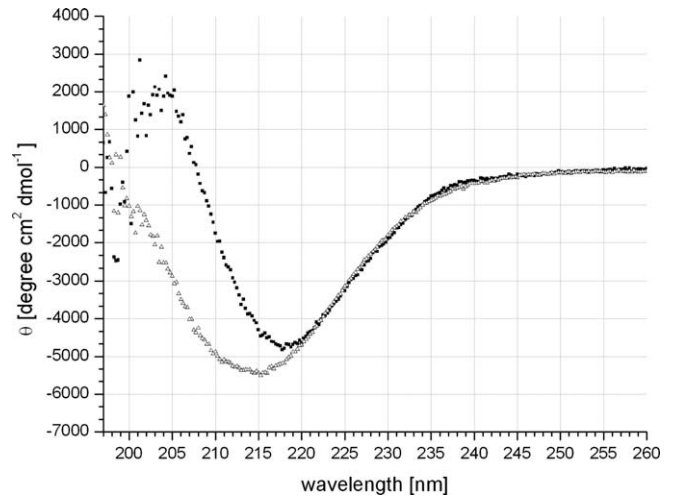


Fig. 8. Far-UV CD spectrum of Ama. Black squares, dimers; open triangles, multimers.

niques. It was previously observed that immobilization on the carbon support and differential staining may both lead to selection of a particular conformation [25,26]. It is not clear whether the Ama multimer particles were distorted/disintegrated by the stain, or whether the experimental conditions for EM selected one conformation preferentially.

Discussion

Until now, studies performed on Ama had been primarily genetic and developmental studies; further characterization and structure determination of this protein in order to understand its homo- and heterophilic binding function requires milligram amounts. Here, we present for the first time recombinant over-expression and subsequent purification of Ama. Since Ama failed to express in soluble form in *E. coli*, most likely due to absence of post-translational modifications, the yeast *P. pastoris* was selected as a eukaryotic expression system. *Pichia* is widely used as an expression system, and has many of the advantages of higher eukaryotic expression systems, such as protein processing, protein folding, and post-translational modification. It is however, faster, easier, and less expensive to use than higher eukaryotic expression systems, such as baculovirus and mammalian cell cultures, and often yields higher expression levels.

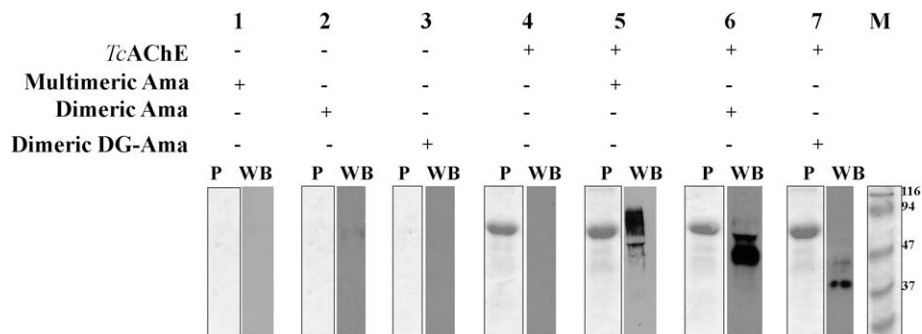


Fig. 7. Interaction of Ama with TcAChE. Ama was captured on an affinity column for TcAChE to which the enzyme had previously been bound, and was coeluted with the enzyme (for details see Materials and methods). The eluate was characterized by Western blotting. For each lane, the nitrocellulose membrane stained with Ponceau red (left) and immunodetection with anti-Ama antibodies (right) are shown. (Lane 1) Control in which the Ama multimer was passed through an affinity column that had not been exposed to TcAChE; (lane 2) control in which the Ama dimer was passed through an affinity column that had not been exposed to TcAChE; (lane 3) control in which DG-Ama was passed through an affinity column that had not been exposed to TcAChE; (lane 4) control in which the affinity column was exposed to TcAChE alone; (lane 5) exposure to TcAChE followed by Ama multimer; (lane 6) exposure to TcAChE followed by the Ama dimer; (lane 7) exposure to TcAChE followed by DG-Ama.

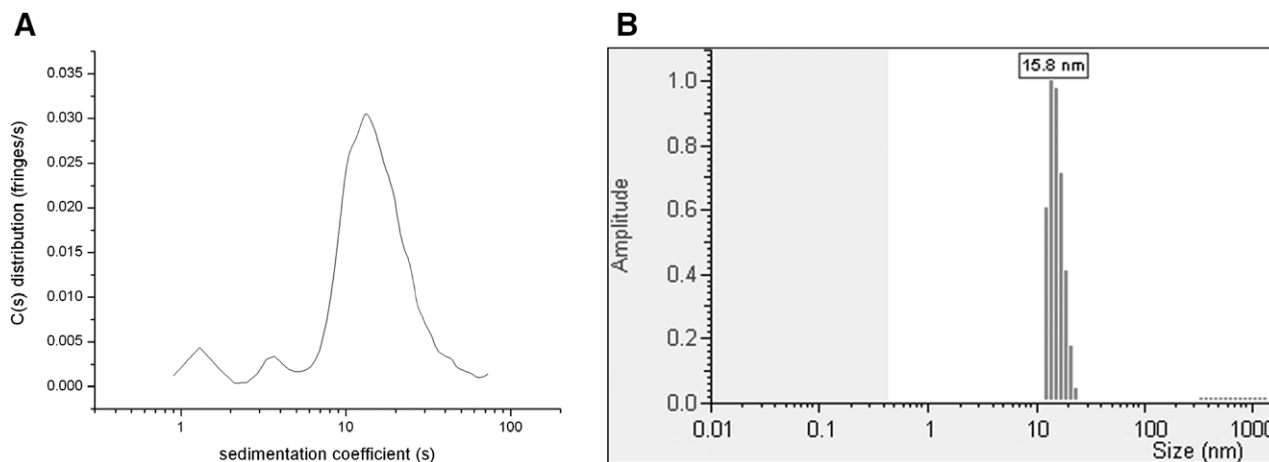


Fig. 9. Size distribution of the Ama multimer fraction. (A) Sedimentation velocity profile. (B) DLS profile.

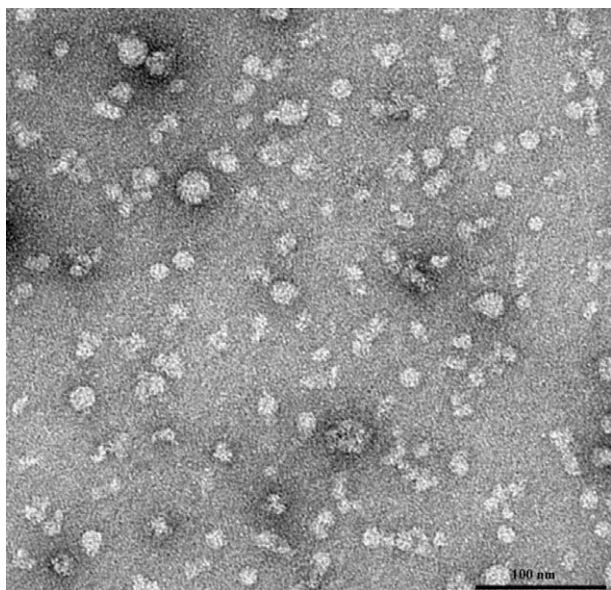


Fig. 10. EM photograph of Ama multimers negatively stained with uranyl acetate.

Ama was secreted in detectable levels by SDS-PAGE from a clone containing multiple copies of the Ama gene. A matrix of conditions, including growth temperature, medium type and pH, was screened for optimal expression conditions, and it was found that expression in buffered medium at pH 5.0 and at 20 °C provided the most satisfactory conditions. Initially, Ama secreted from *Pichia* was found to be expressed primarily as high-order multimers. By analyzing aliquots taken directly from the growth medium it was shown that the multimers are formed prior to purification. Two protocols were examined for reducing multimer formation during expression of Ama in *Pichia*. It was shown that *Pichia* is able to grow in the presence of substantial concentrations of the zwitterionic detergent CHAPS, and that under such conditions the bulk of the Ama is expressed as dimers. However, the presence of the detergent lowers overall expression levels of Ama. The alternative procedure of gradually lowering the rate of agitation and reducing the air/liquid interfacial foam area in the shaking flask also lowered the percentage of multimers. Although the percentage of the Ama dimer was lower in this latter procedure, overall levels of dimer were higher than obtained in the presence of CHAPS, and it was thus adopted as the preferred procedure for its expression. In addition,

by daily monitoring of the pH it was observed that the pH of the BMM drops to pH 2.5 after 72 h of induction, which did not occur in BMMY (data not shown). Since some Ig-domain proteins have been shown to denature at low pH values [6,27], we selected BMMY, pH 5.0, as the preferred medium for expression and subsequent purification of Ama.

The functionality of the recombinant Ama was validated by the experiment in which, when co-expressed with Nrt-ext, its native receptor [7], the two were clearly shown to interact (Fig. 6). Furthermore, in an interaction experiment performed making use of an affinity column for purification of AChE, it was shown that the two fractions of Ama, viz., the multimeric and the dimeric, both interact with TcAChE. This supports the earlier findings of Darboux and coworkers who showed that a chimera in which the extracellular cholinesterase-like domain of Nrt had been replaced by TcAChE retained its biological activity [23]. It was further shown that Ama could bind to TcAChE even when its glycans were removed, indicating the glycans are not involved in the interaction. These results also suggest that Ama does not bind to AChE in the region of the entrance to the active-site gorge, since if this were the case Ama would either not have interacted at all with the TcAChE bound to the affinity column or, by competing with the ligand on the affinity column, would have eluted the bound enzyme. This is in agreement with the assignment of Frémion et al. [7], who presented data suggesting that residues 347–482 on Nrt are necessary for Ama binding, and do not overlap with the region corresponding to the entrance of the active-site gorge in AChE.

The solubility and stability (viz., their failure to dissociate) of the Ama multimers permitted their biophysical characterization and visualization by EM. It should be noted that upon SDS-PAGE under non-reducing conditions no evidence for occurrence of disulfide-linked dimers or multimers was obtained (not shown). All the techniques employed showed that they are not non-specific protein aggregates. Far-UV CD showed that they possess substantial β -sheet secondary structure, but with higher random coil content than the dimers, whose CD spectrum is typical of IgSF proteins [28]. Furthermore the two biophysical techniques employed, viz., DLS and AUC-SV, are in reasonable agreement with respect to the dimensions of the multimers.

The modes of interaction of Ig-type cell adhesion molecules, which usually contain several Ig domains, are currently less well understood than those of other cell adhesion molecules, such as the integrins and cadherins [29]. One functional model, however, has emerged from studies of the neuronal cell adhesion molecule, L1 [30], the neural adhesion receptor axonin/TAG-1 [31] and the insect adhesion protein hemolin [32], which are structurally re-

lated. The crystal structure of the hemolin monomer, which contains 4 Ig domains, reveals a horseshoe structure in which domain 1 interacts with domain 4, and domain 2 with domain 3. Bjorkman and colleagues proposed that this bent conformation represents a 'closed' or self-inhibited form of hemolin [32], and that an open form, in which the hinge loop between domain 2 and 3 is extended, would allow for precisely the same interdomain interactions; but rather than being intramolecular, they would be intermolecular, between domains of separate hemolin molecules presented by juxtaposed membrane surfaces. This mode of binding is an example of 3D domain swapping [33], which was also found to be a mechanism utilized by members of the cadherin family [34]. In such domain swapping, either an individual secondary structure element is swapped, as in the case for the cadherins, or a whole domain is swapped, as in the case for hemolin. In another Ig-domain-containing protein, domain swapping was suggested as a mechanism for multimerization. Single-chain Fv (scF_v) molecules are recombinant antibody fragments consisting of only two Ig domains [35], which form monomers, dimers, and higher oligomers in solution. The X-ray structure of the scF_v dimer showed that it is formed by domain swapping [36].

Based on the reported ability of Ig multi-domain proteins to oligomerize via the domain swapping mechanism mentioned above, we suggest that Ama multimers may be formed similarly. The ability to produce and purify two different forms of Ama (dimeric and multimeric) will permit further structural studies on these two forms to verify the domain swapping mechanism hypothesis for Ama. Such studies may enhance our understanding the mode of action of Ig-type cell adhesion molecules in general and in axon guidance in particular.

Acknowledgments

The authors are grateful to Nurit Levy for help in expression of Ama in *Pichia* and to Dr. Michel Piovant for the amalgam and neurotactin cDNAs. The EM studies were conducted in the Irving and Cherna Moskowitz Center for Nano and Bio-Nano Imaging at the Weizmann Institute of Science. This study was supported by the Israel Science Foundation, Autism Speaks, the European Commission Sixth Framework Research and Technological Development Program 'SPINE2-COMPLEXES' Project, under contract No. 031220 and 'Teach-SG' Project, under contract No. ISSG-CT-2007-037198, the Kimmelman Center for Biomolecular Structure and Assembly (Rehovot, Israel), the Benozio Center for Neurosciences, the Divadol Foundation, the Nalvyco Foundation, the Bruce Rosen Foundation, the Jean and Julia Goldwurm Memorial Foundation, the Neuman Foundation, and the Kalman and Ida Wolens Foundation. J.L.S. is the Morton and Gladys Pickman Professor of Structural Biology.

References

- [1] G. Apic, J. Gough, S.A. Teichmann, Domain combinations in archaeal, eubacterial and eukaryotic proteomes, *J. Mol. Biol.* 310 (2001) 311–325.
- [2] C.F. Wright, S.A. Teichmann, J. Clarke, C.M. Dobson, The importance of sequence diversity in the aggregation and evolution of proteins, *Nature* 438 (2005) 878–881.
- [3] P. Smailowski, A.J. Martin-Galiano, A. Mikolajka, T. Girschick, T.A. Holak, D. Frishman, Protein solubility: sequence based prediction and experimental verification, *Bioinformatics* 23 (2007) 2536–2542.
- [4] M.A. Seeger, L. Haffley, T.C. Kaufman, Characterization of amalgam: a member of the immunoglobulin superfamily from *Drosophila*, *Cell* 55 (1988) 589–600.
- [5] A.F. Williams, A.N. Barclay, The immunoglobulin superfamily-domains for cell surface recognition, *Ann. Rev. Immunol.* 6 (1988) 381–405.
- [6] P.O. Souillac, V.N. Uversky, I.S. Millett, R. Khurana, S. Doniach, A.L. Fink, Effect of association state and conformational stability on the kinetics of immunoglobulin light chain amyloid fibril formation at physiological pH, *J. Biol. Chem.* 277 (2002) 12657–12665.
- [7] F. Frémion, I. Darboux, M. Diano, R. Hipeau-Jacquotte, M.A. Seeger, M. Piovant, Amalgam is a ligand for the transmembrane receptor neurotactin and is required for neurotactin-mediated cell adhesion and axon fasciculation in *Drosophila*, *EMBO J.* 19 (2000) 4463–4472.
- [8] S. de la Escalera, E.O. Bockamp, F. Moya, M. Piovant, F. Jimenez, Characterization and gene cloning of neurotactin, a *Drosophila* transmembrane protein related to cholinesterases, *EMBO J.* 9 (1990) 3593–3601.
- [9] Y. Barthalay, R. Hipeau-Jacquotte, S. de la Escalera, F. Jimenez, M. Piovant, *Drosophila* neurotactin mediates heterophilic cell adhesion, *EMBO J.* 9 (1990) 3603–3609.
- [10] T. Zeev-Ben-Mordehai, E.H. Rydberg, A. Solomon, L. Toker, V.J. Auld, I. Silman, S. Botti, J.L. Sussman, The intracellular domain of the *Drosophila* cholinesterase-like neural adhesion protein, gliotactin, is natively unfolded, *Proteins* 53 (2003) 758–767.
- [11] E.C. Liebl, R.G. Rowe, D.J. Forsthoefel, A.L. Stammler, E.R. Schmidt, M. Turski, M.A. Seeger, Interactions between the secreted protein Amalgam, its transmembrane receptor Neurotactin and the Abelson tyrosine kinase affect axon pathfinding, *Development* 130 (2003) 3217–3226.
- [12] J.L. Sussman, M. Harel, F. Frolow, L. Varon, L. Toker, A.H. Futerman, I. Silman, Purification and crystallization of a dimeric form of acetylcholinesterase from *Torpedo californica* subsequent to solubilization with phosphatidylinositol-specific phospholipase C, *J. Mol. Biol.* 203 (1988) 821–823.
- [13] L.D. Cabrita, D. Gilis, A.L. Robertson, Y. Dehouck, M. Rooman, S.P. Bottomley, Enhancing the stability and solubility of TEV protease using in silico design, *Protein Sci.* 16 (2007) 2360–2367.
- [14] J.J. Clare, M.A. Romanos, F.B. Rayment, J.E. Rowedder, M.A. Smith, M.M. Payne, K. Sreekrishna, C.A. Henwood, Production of mouse epidermal growth factor in yeast: high-level secretion using *Pichia pastoris* strains containing multiple gene copies, *Gene* 105 (1991) 205–212.
- [15] F. Grueninger-Leitch, A. D'Arcy, B. D'Arcy, C. Chene, Deglycosylation of proteins for crystallization using recombinant fusion protein glycosidases, *Protein Sci.* 5 (1996) 2617–2622.
- [16] P. Schuck, P. Rossmanith, Determination of the sedimentation coefficient distribution by least-squares boundary modeling, *Biopolymers* 54 (2000) 328–341.
- [17] T.M. Laue, B.D. Shah, T.M. Ridgeway, S.L. Pelletier, Analytical Ultracentrifugation in Biochemistry and Polymer Science, The Royal Society of Chemistry, Cambridge, 1992.
- [18] K. Sreekrishna, R.G. Brankamp, K.E. Kropp, D.T. Blankenship, J.T. Tsay, P.L. Smith, J.D. Wierschke, A. Subramaniam, L.A. Birkenberger, Strategies for optimal synthesis and secretion of heterologous proteins in the methylotrophic yeast *Pichia pastoris*, *Gene* 190 (1997) 55–62.
- [19] Y. Hao, J. Chu, Y. Wang, Y. Zhuang, S. Zhang, The inhibition of aggregation of recombinant human consensus interferon- α mutant during *Pichia pastoris* fermentation, *Appl. Microbiol. Biotechnol.* 74 (2007) 578–584.
- [20] J.H. Woo, Y.Y. Liu, D.M. Neville Jr., Minimization of aggregation of secreted bivalent anti-human T cell immunotoxin in *Pichia pastoris* bioreactor culture by optimizing culture conditions for protein secretion, *J. Biotechnol.* 121 (2006) 75–85.
- [21] J.M. Cregg, J.L. Cereghino, J. Shi, D.R. Higgins, Recombinant protein expression in *Pichia pastoris*, *Molec. Biotech.* 16 (2000) 23–52.
- [22] R.K. Bretthauer, F.J. Castellino, Glycosylation of *Pichia pastoris*-derived proteins, *Biotechnol. Appl. Biochem.* 30 (Pt 3) (1999) 193–200.
- [23] I. Darboux, Y. Barthalay, M. Piovant, R. Hipeau-Jacquotte, The structure-function relationships in *Drosophila* neurotactin show that cholinesterase domains may have adhesive properties, *EMBO J.* 15 (1996) 4835–4843.
- [24] P.M. Bayley, Circular dichroism and optical rotation, in: S.B. Brown (Ed.), *An Introduction to Spectroscopy for Biochemists*, Academic Press, London, 1980, pp. 148–235.
- [25] M. Pioletti, F. Findeisen, G.L. Hura, D.L. Minor Jr., Three-dimensional structure of the KChIP1-Kv4.3 T1 complex reveals a cross-shaped octamer, *Nat. Struct. Mol. Biol.* 13 (2006) 987–995.
- [26] H. Tidow, R. Melero, E. Mylonas, S.M. Freund, J.G. Grossmann, J.M. Carazo, D.I. Svergun, M. Valle, A.R. Fersht, Quaternary structures of tumor suppressor p53 and a specific p53 DNA complex, *Proc. Natl. Acad. Sci. USA* 104 (2007) 12324–12329.
- [27] P.O. Souillac, V.N. Uversky, I.S. Millett, R. Khurana, S. Doniach, A.L. Fink, Elucidation of the molecular mechanism during the early events in immunoglobulin light chain amyloid fibrillation. Evidence for an off-pathway oligomer at acidic pH, *J. Biol. Chem.* 277 (2002) 12666–12679.
- [28] G.W. Litman, R.A. Good, D. Frommel, A. Rosenberg, Conformational significance of the intrachain disulfide linkages in immunoglobulins, *Proc. Natl. Acad. Sci. USA* 67 (1970) 1085–1092.
- [29] L. Shapiro, J. Love, D.R. Colman, Adhesion molecules in the nervous system: structural insights into function and diversity, *Annu. Rev. Neurosci.* 30 (2007) 451–474.
- [30] G. Schurmann, J. Haspel, M. Grumet, H.P. Erickson, Cell adhesion molecule L1 in folded (horseshoe) and extended conformations, *Mol. Biol. Cell.* 12 (2001) 1765–1773.
- [31] J. Freigang, K. Proba, L. Leder, K. Diederichs, P. Sonderegger, W. Welte, The crystal structure of the ligand binding module of axonin-1/TAG-1 suggests a zipper mechanism for neural cell adhesion, *Cell* 101 (2000) 425–433.
- [32] X.D. Su, L.N. Gastinel, D.E. Vaughn, I. Faye, P. Poon, P.J. Bjorkman, Crystal structure of hemolin: a horseshoe shape with implications for homophilic adhesion, *Science* 281 (1998) 991–995.

- [33] M.P. Schlunegger, M.J. Bennett, D. Eisenberg, Oligomer formation by 3D domain swapping: a model for protein assembly and misassembly, *Adv. Protein Chem.* 50 (1997) 61–122.
- [34] C.P. Chen, S. Posy, A. Ben-Shaul, L. Shapiro, B.H. Honig, Specificity of cell-cell adhesion by classical cadherins: critical role for low-affinity dimerization through beta-strand swapping, *Proc. Natl. Acad. Sci. USA* 102 (2005) 8531–8536.
- [35] R. Raag, M. Whitlow, Single-chain Fvs, *FASEB J.* 9 (1995) 73–80.
- [36] A.A. Kortt, R.L. Malby, J.B. Caldwell, L.C. Gruen, N. Ivancic, M.C. Lawrence, G.J. Howlett, R.G. Webster, P.J. Hudson, P.M. Colman, Recombinant anti-sialidase single-chain variable fragment antibody. Characterization, formation of dimer and higher-molecular-mass multimers and the solution of the crystal structure of the single-chain variable fragment/sialidase complex, *Eur. J. Biochem.* 221 (1994) 151–157.